SAR-based Wind Resource Statistics in the Baltic Sea

Hasager, Charlotte Bay; Badger, Merete; Pena Diaz, Alfredo; Larsén, Xiaoli Guo; Bingöl, Ferhat

Published in:
Remote Sensing

Link to article, DOI:
10.3390/rs3010117

Publication date:
2011

Document Version
Publisher's PDF, also known as Version of record

Remote Sens. **2011**, *3*, 117-144; doi:10.3390/rs3010117

OPEN ACCESS

Remote Sensing

ISSN 2072-4292

www.mdpi.com/journal/remotesensing

Article

SAR-Based Wind Resource Statistics in the Baltic Sea

Charlotte B. Hasager *, Merete Badger, Alfredo Peña, Xiaoli G. Larsén and Ferhat Bingöl

Wind Energy Division, Risø DTU, Frederiksborgvej 399, 4000 Roskilde, Denmark;
E-Mails: mebc@risoe.dtu.dk (M.B.); aldi@risoe.dtu.dk (A.P.); xgal@risoe.dtu.dk (X.L.);
febi@risoe.dtu.dk (F.B.)

* Author to whom correspondence should be addressed; E-Mail: cbha@risoe.dtu.dk;
Tel.: +45-4677-5014; Fax: +45-4677-5970.

Received: 16 November 2010; in revised form: 22 December 2010 / Accepted: 31 December 2010 / Published: 11 January 2011

Abstract: Ocean winds in the Baltic Sea are expected to power many wind farms in the coming years. This study examines satellite Synthetic Aperture Radar (SAR) images from Envisat ASAR for mapping wind resources with high spatial resolution. Around 900 collocated pairs of wind speed from SAR wind maps and from 10 meteorological masts, established specifically for wind energy in the study area, are compared. The statistical results comparing *in situ* wind speed and SAR-based wind speed show a root mean square error of 1.17 m s^{-1}, bias of −0.25 m s^{-1}, standard deviation of 1.88 m s^{-1} and correlation coefficient of R^2 0.783. Wind directions from a global atmospheric model, interpolated in time and space, are used as input to the geophysical model function CMOD-5 for SAR wind retrieval. Wind directions compared to mast observations show a root mean square error of 6.29° with a bias of 7.75°, standard deviation of 20.11° and R^2 of 0.950. The scale and shape parameters, A and k, respectively, from the Weibull probability density function are compared at only one available mast and the results deviate ~2% for A but ~16% for k. Maps of A and k, and wind power density based on more than 1000 satellite images show wind power density values to range from 300 to 800 W m^{-2} for the 14 existing and 42 planned wind farms.

Keywords: offshore wind; satellite SAR; wind energy; wind resource

---

1. Introduction

Satellite Synthetic Aperture Radar (SAR) can be used for ocean wind mapping at high spatial resolution. The study aims to verify the applicability of the SAR-based method for wind resource mapping in part of the Baltic Sea. Firstly, SAR-based wind maps are compared to observations from 10 meteorological *in situ* masts using around 900 collocations. Thereafter, an offshore wind resource map is calculated using SAR-based wind maps. Finally, wind resource statistics observed at one site are compared to the SAR-based results, and the wind resource results from existing and planned offshore wind farms are examined.

Several studies demonstrate that C-band SAR (~5.3 GHz) can be used to extract wind speed and wind direction over the ocean at high spatial resolution ~1 km × 1 km [1-6]. In the present study, data from the Advanced SAR (ASAR), on-board the Envisat satellite launched in 2002 by the European Space Agency (ESA), are investigated. The ASAR provide several modes, one of them the wide swath mode (WSM) with 400 km swath. The specific advantage of the Envisat ASAR WSM is the excellent coverage in the study area, the southwestern part of the Baltic Sea including parts of the Danish, Swedish, German and Polish waters covering the area from 10° to 19°E longitude and 54° to 58°N latitude. Kattegat Strait is included. See Figure 1.

Figure 1. Map of the study area with indication of the 17 meteorological masts. Those indicated with ◊ are used in the comparison study.

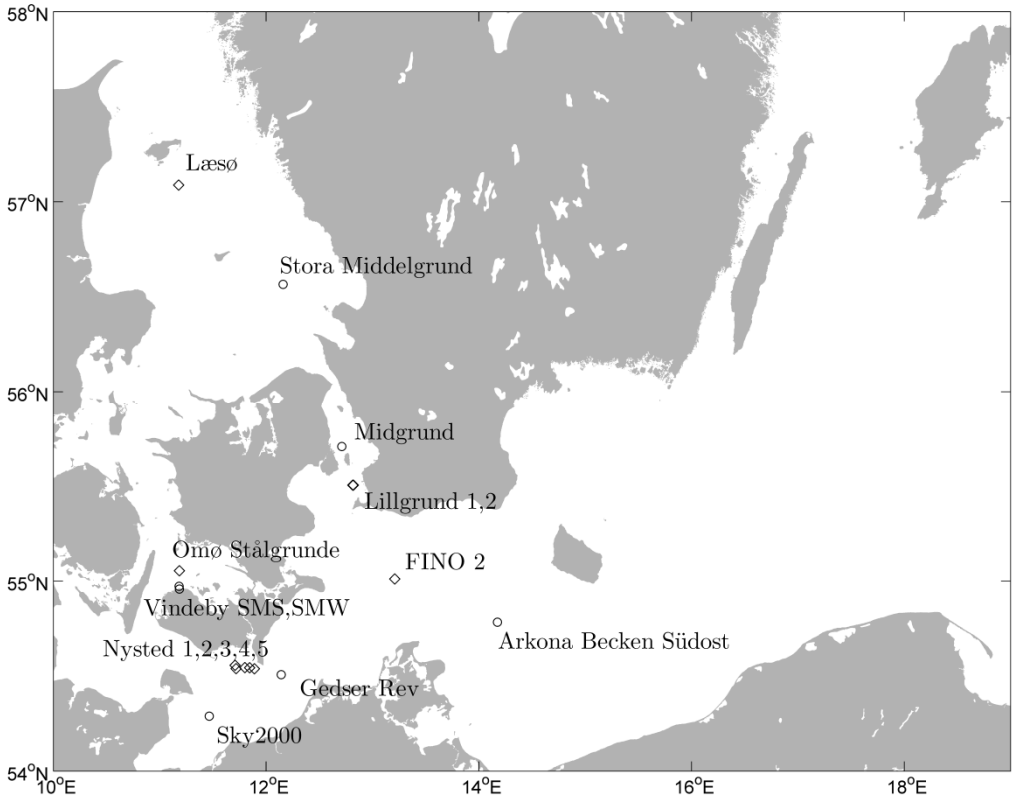

Offshore wind power began at Vindeby in 1992 with 11 wind turbines located in the Baltic Sea in Denmark. The installed capacity of this first wind farm is ~5 MW. Today the study area in the Baltic Sea is home to 14 wind farms with a total capacity of 622 MW distributed as 486 MW in Denmark,

133 MW in Sweden and 3 MW in Germany. There are plans to increase to a total of 12 GW offshore wind farm capacity in the Baltic Sea within the study area. The plans include new capacities in Denmark 1,854 MW, Sweden 5,218 MW, Germany 3,540 MW and Poland 900 MW, see Appendix A for details. In the Baltic Sea outside the study area there are offshore wind farm plans in Estonia, Latvia, Lithuania, Russia (Kaliningrad), Finland and Sweden. Thus there is interest in offshore wind statistics in the Baltic Sea. Predictions on wind resources for the new wind farm sites are interesting.

Satellite SAR used in wind resource estimation has a brief history having started at the turn of the Millennium [7]. Satellite SAR wind maps from the North Sea have been compared to meteorological mast data [8-10]. Satellite-based SAR wind mapping in the Baltic Sea encompasses the wind farm wake study near the Nysted wind farm [11], case studies comparing satellite SAR and mesoscale model results [1,12-14], and the production of preliminary mean wind speed maps without comparison to *in situ* data or model results [15,16].

Observing offshore winds with meteorological masts is costly, but at least 17 masts have been installed within the study area of the southern Baltic Sea, and the Skagerrak and Kattegat Straits. The novelty of the present study is the inclusion of ten different meteorological masts—all installed for the specific purpose of wind resource assessment—enabling a comprehensive comparison within the study area. It is anticipated that the quality of the meteorological observations will be of higher precision and accuracy than buoy wind data. The comparison is done case by case, on wind speed using a footprint averaging technique in the SAR-based wind maps and a time-average from the mast data.

The article describes satellite SAR wind mapping, the meteorological data from the masts, and the comparison results on wind speed, wind direction and wind resource statistics. Furthermore, the wind resource map based on more than 1,000 wind maps and wind resource statistics for present and future offshore wind farms in the study area of the Baltic Sea are presented and the results are discussed.

2. Satellite SAR Wind Mapping

In the Wind Energy Division at Risø DTU satellite, SAR wind mapping is performed using the Johns Hopkins University, Applied Physics Laboratory (JHU/APL) software APL/NOAA SAR Wind Retrieval System (ANSWRS). The Envisat ASAR WSM images are downloaded in near-real-time from ESA and the following automated procedure is applied: The pixels are calibrated to obtain the Normalized Radar Cross-Section (NRCS) value, then pixels are averaged to around 500 m, and finally the geophysical model function CMOD-5 [17] is used to retrieve wind speed using the wind direction *a priori* from the US Navy Operational Global Atmospheric Prediction System (NOGAPS). The spatial averaging of SAR pixels suppresses noise effects from longer ocean waves and from speckle, an inherent property of imaging radars. The 6-hourly model wind vectors are available at a 1 degree latitude and longitude grid and the wind vectors from the lowest model level around 10 m above the surface are used. To match the satellite data, the wind vectors are interpolated in time and space [18,19].

The wind maps resolve details on atmospheric mesoscale wind phenomena. Figure 2 shows the wind speed map from 1 January 2010 observed at 20.48 UTC. All time stamps in the article are in UTC. In Skagerrak Strait strong winds are channeled between Norway and Denmark from the northeast. Wind streaks are present and wind speeds are between 15 and 20 m s^{-1}. In the South Baltic

Sea the winds are weaker, around 7 to 12 m s^{-1} with lee effects southwest of the Danish islands and along the Swedish coast.

Figure 2. Wind speed map of the South Baltic Sea and interior Danish Seas observed from Envisat ASAR wide swath mode on 1 January 2010 at 20.48 UTC with the NOGAPS wind direction vectors shown in white. Risø DTU/JHU APL.

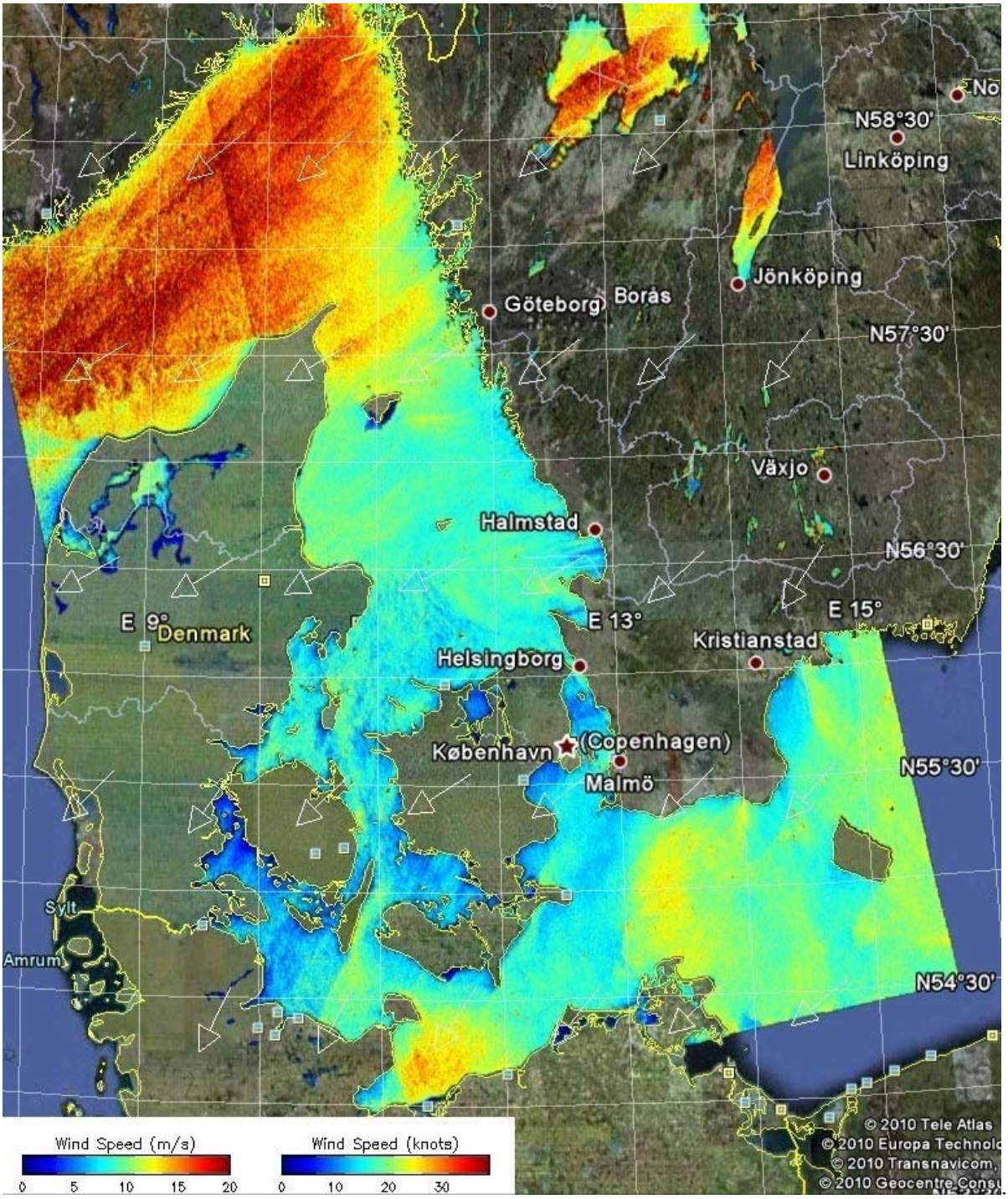

The microwave radiation backscattered from the ocean surface is non-linearly proportional to the size and orientation of capillary and short-gravity waves produced near-instantaneously by the local surface winds. Thus using information on the radar incidence, azimuth angle, and relative wind

direction, the wind speed is retrieved for a neutrally stratified marine atmosphere at 10 m a.s.l. from the empirical CMOD functions. A more detailed description of SAR-based wind retrieval is given in [15]. In near-coastal regions non-neutral static stratification often prevails, and a correction to the neutral wind profile would be ideal. However, for this task accurate sea and air temperatures are necessary, and this information is generally not available.

Physical obstacles located in the ocean such as ships, oil rigs, and wind turbines act as reflectors and the backscattered microwave radiation is significantly increased. The CMOD function will, in such cases, provide a positively biased wind speed observation. In contrast, oil spill and thick algae blooms at the ocean surface can reduce the backscattered signal as the generation of capillary waves is hindered. The result is a negatively biased wind speed. Convective rain cells also influence SAR data. Often a pattern is seen with increased winds around the rain cell, and with reduced wind inside the rain cell, possibly due to the rain drop's interference (splashing effect) with the capillary waves and/or lower winds. Sea bottom structures, ocean and tidal currents [20], and long internal ocean waves can also influence SAR and override the basic wind speed signal. For the study area one or more of the above situations may occur. However, despite all these possible shortcomings, ocean winds are generally mapped reasonably well from C-band SAR [6]. Sea ice was present in parts of the study area from late January to late February 2010 as it was an unusually cold winter. Information from the Swedish Meteorological and Hydrological Institute (SMHI) Ice Service and visual inspection of the wind maps were used to discard some scenes.

At Risø DTU 1009 Envisat ASAR WSM scenes covering the study area are processed to wind maps. Table 1 lists the number of scenes per year and per month. There are 523 morning passes observed between 08.52 and 10.01 UTC and 486 evening passes observed between 20.05 and 21.06 UTC.

Table 1. Envisat ASAR data used in the study per year and per month.

Year	**2003**	**2004**	**2005**	**2006**	**2007**	**2008**	**2009**	**2010**
Number of scenes	8	30	10	115	302	246	248	50

Month	**1**	**2**	**3**	**4**	**5**	**6**	**7**	**8**	**9**	**10**	**11**	**12**
Number of scenes	102	69	119	63	76	64	83	79	97	81	77	99

Footprint Averaging and Wind Resource Statistics

The comparison of SAR-based winds to meteorological wind observations is done using footprint averaging in the wind maps. The footprint theory [21] as described in [22] is used. The footprint is located upwind of each meteorological mast in each collocated wind map. The wind direction is used locally to estimate the direction of the footprint. The size of the footprint is a function of the height, which in this case is 10 m above sea level. The pixels within the 95% limit of the footprint are split into very tiny areas and each area is weighted with the footprint density function and averaged. In this way a physically-based selection of spatial wind information is used according to atmospheric theory to compare winds at a certain position (x,y,z,t) in time. For a roughness at sea around 0.0002 m the

footprint stretches around 860 m upwind with the maximum influence at half this distance. The statistical analysis of SAR wind maps is performed with the Satellite-Wind Atlas Analysis and Application Program (S-WAsP) tool developed by Risø DTU [23].

The Weibull probability distribution function is commonly used to describe wind speed data as in the European Wind Atlas [24]. The available wind power density, E, (that is proportional to the wind speed cubed), may be calculated from the two Weibull parameters, the scale parameter A and the shape parameter k, using the gamma function Γ, and the air density ρ (~1.245 g/m^3 at 10 °C) as

$$\mathrm{E} = \frac{1}{2}\rho A^3 \Gamma\left(1+\frac{3}{k}\right). \quad (1)$$

Studies from the North Sea have shown SAR wind maps to be a possible source of information for the estimation of A and k [8,10]. Recent results from the North Sea show deviations between SAR-based wind resource statistics compared to the meteorological data below 5% for the mean wind speed and A and below 7% for E and k, when a sufficient number of samples are available [10]. If only 100 to 200 samples can be purchased the new wind class method is recommended. It is necessary to have many more available images in the data archive in order to populate the wind classes. The wind class method is based on a selection of SAR wind maps for the analysis combined with weighting of the SAR-based results using long-term mesoscale model statistics as input to quantify the weighting coefficients. The wind class method is primarily relevant when few samples are available whereas if more than 400 samples are available the random sampling method appears to be the best option. The random sampling method is based on equal weight to all available samples. This is used here. Weibull fitting of the SAR-based wind maps is done with the maximum likelihood estimator suitable for sparse data sets [25].

3. Meteorological Data

The locations of the 17 meteorological masts are indicated in Figure 1. Table 2 lists the geographical coordinates of the met-masts and the data owners. The data periods with the first and last observation from each of the ten masts used in the comparison study and the observational heights are listed. Data from the other seven masts are not available or do not overlap in time with the satellite images, however, basic information on these masts is also included in Table 2.

Brief descriptions of the meteorological data and data analysis for each of the ten meteorological masts are given in Sections 3.1 to 3.5. It is the wind speed at 10 m above sea level that is extracted from satellite SAR, thus it has been chosen to extrapolate the met-mast wind speed to this height—if not directly observed at 10 m. In order for the statistics from the masts to match well with the footprint averaging technique, an hourly average centered at the satellite recording time is used. At shorter averaging time scales, e.g., 10 minutes, greater scatter is found, probably because the finer scales are not resolved in SAR. All masts have data stored every 10 minutes and several masts have two-sided measurements (to avoid mast shadow effects).

Table 2. Longitude (long.) and latitude (lat.) for 17 met-masts in the study area: *In situ* data from the top ten masts are used in the comparison study with indication of the data periods used and the observational heights for wind speed (z_u in m) (some two-sided) and direction (z_{dir} in m) used. The distance (D in km) to nearest land is given for all masts.

Met mast	Long. Lat.	Owner	Period	Country	D	z_u	z_{dir}
FINO-2	13.154167, 55.006944	BMU*	20071209 20090921	DE	38.2	32 to 102 at 8 heights	32
Lillgrund-1	12.760000, 55.500000	Vattenfall	20031010 20050902	SE	8.7	25 (N/S)	23
Lillgrund-2	12.765400, 55.499783	Vattenfall	20060531 20071228	SE	8.7	13	18
Læsø	11.123250, 57.08422	Techwise	20030301 20031010	DK	13.9	15 (SW/NE)	28
Nysted-1	11.663461, 54.53527	DONG Energy	20040620 20080610	DK	7.1	10	10
Nysted-2	11.654026, 54.55354	DONG Energy	20040617 20080404	DK	7.3	10	10
Nysted-3	11.790082, 54.53981	DONG Energy	20040620 20080607	DK	9.2	10	10
Nysted-4	11.835698, 54.53494	DONG Energy	20040620 20080607	DK	6.9	10	10
Nysted-5	11.745960, 54.54075	DONG Energy	20030301 20050524	DK	11.8	8	44
Omø Stålgrunde	11.130000, 55.050000	DONG Energy	20030301 20050524	DK	10.4	10	48
Arkona Becken SÖ	14.12, 54.78	Arkona-Windpark	2007–	DE	37.1		
Gedser Rev	12.086800, 54.503250	Risø DTU	1997–2003	DK	9.5		
Midgrund	12.657122, 55.702861	Risø DTU	1997–1999	DK	2.3		
Sky2000	11.410367, 54.285115	GEOmbH	2003–	DE	14.7	No data used	
Stora Middelgrund	12.104708, 56.561347	Universal WindOffshore	2008–2009	SE	29.7		
Vindeby SMS	11.130053, 54.954461	Risø DTU	1993–2001	DK	0.3		
Vindeby SMW	11.127326, 54.968162	Risø DTU	1993–1998	DK	1.7		

*BMU: Federal Ministry for the Environment, Nature Conservation and Nuclear Safety in Germany.

Six of the meteorological masts are located near offshore wind farms and observe wind farm wake effects for certain wind directions, *i.e.*, reduced wind speeds. In the context of comparing wake-influenced meteorological data and wake-influenced satellite SAR, it is expected that the satellite wind maps record similarly reduced wind speeds. Only when satellite backscatter is enhanced, due to returns from the turbine towers and blades, an apparent too high wind speed is expected. The footprint has a length of around 860 m. Wind speed data are omitted from the verification study (but presented in a separate table) when wind turbines are positioned closer to the mast than this distance.

3.1. FINO-2 Data

The FINO-2 meteorological mast is the second of the three German 'Forschungs-plattformen in Nord- und Ostsee' (research platforms in the North and Baltic Seas). It is located midway between Germany and Sweden, around 38.2 km and 38.6 km, respectively. Information is available at http://212.201.38.20/fino2/. The wind speed at 32, 42, 52, 62, 72, 82, 92, 102 m is extrapolated to 10 m using the logarithmic wind profile and the Charnock roughness model with the constant set at 0.0144 following [26] and assuming neutral stability. There is no wind farm nearby.

3.2. Lillgrund-1/-2 Data

The Lillgrund-1 data were collected prior to construction of the Lillgrund wind farm that consists of 48 turbines of 2.3 MW. Wind speed observations at 25 m height at two booms in directions north and south are used. The highest wind speed from the two booms is selected to avoid mast shadow effects. The wind speed is extrapolated to 10 m as for FINO-2.

The Lillgrund-2 mast is in fact the Lillgrund-1 mast moved to a nearby location and re-instrumented. The Lillgrund wind farm is constructed less than 500 m east of the Lillgrund-2 meteorological mast. This results in a wind farm wake sector from 300° to 360° and 0° to 120°, and a free stream wind sector from 120° to 300°. Only the free stream sector is useful for wind speed verification analysis. The wind speed is observed at 13 m and extrapolated to 10 m as for FINO-2.

3.3. Læsø Data

The Læsø data were recorded in the early years of the Envisat mission. Only a few SAR observations are collocated with mast data in our dataset. The wind speed is observed at 15 m at two booms pointing southwest and northeast. The highest wind speed is selected to avoid mast shadow effects, and the data are extrapolated to 10 m as for FINO-2. There is no wind farm nearby.

3.4. Nysted-1/-2/-3/-4/-5 Data

The five meteorological masts at Nysted are located near the Nysted offshore wind farm. For the layout of the wind farm and masts see [27] and http://www.dongenergy.com/Nysted. Only meteorological observations after construction of the wind farm are used in the study. The Nysted wind farm started to operate on the 1 December 2003. Two of the masts, Nysted-1/-2, are located west of the wind farm both at distances of less than 500 m from the nearest row of wind turbines. The two other masts, Nysted-3/-4, are located east of the wind farm at distances of around 1 km and 4 km,

respectively, from the nearest row of wind turbines. The fifth mast, Nysted-5, is located within the wind farm itself. The position of the masts and the wind turbines, results in the following wake and free stream sectors: Nysted-1/-2 both have wake sectors from 0° to 180° and free stream sectors from 180° to 360°. Nysted-3 and -4 are located far enough from the wind farm to have free stream sector for all 360°. This only implies that the upwind footprint of the satellite SAR is shorter than the distance to the nearest wind turbines and the turbines do not contribute high backscatter. Nysted-5 is located inside the wind farm and has a 360° wake influenced sector.

At Nysted-1/-2/-3/-4, wind speeds are measured with cup anemometers at heights above mean sea level of 10 m and up to 69 m and wind directions are measured at 10 m and 65 m. At Nysted-5, wind speeds are measured at 8 m and 44 m and direction at 44 m; here the wind speed at 10 m is extrapolated from that at 8 m, by using the Charnock formulation for the surface roughness length. Due to the short distance—here 2 m—the stability effect is neglected.

The study of [13] shows that over the water area where the Nysted wind farm is, the stability parameter, the Richardson number R_i, is larger than zero for about 61% of the time and about 26% of the time it is strongly stable with $R_i > 0.25$, suggesting mainly stable conditions. These features are in agreement with the studies of [28] and [29], where it was also shown that throughout most of the year, the atmosphere over the Baltic Sea is stable. This stable condition indicates a source of uncertainty in the SAR wind retrievals where neutral stability is assumed.

3.5. Omø Stålgrunde Data

The Omå Stålgrunde mast observes wind speeds at 10 m. There is no wind farm nearby.

3.6. Wind Direction from All Masts

Wind directions in the wind maps are from the NOGAPS model. The wind direction is reported both for free stream and wake influence sectors. Wind direction is poorly defined for very low wind speeds. Wind direction comparison results are reported only for cases of wind speed larger than 3 m s^{-1} observed in the SAR wind maps. Wind direction in NOGAPS is from the lowest model layer, around 10 m above surface. For the masts the wind directions are observed at the following heights: FINO-2 at 32 m, Lillgrund-1 at 23 m, Lillgrund-2 at 18 m, Læsø at 28 m, Nysted-1/-2/-3/-4 at 10 m, Nysted-5 at 44 m, and Omø Stålgrunde at 48 m. The wind directions from the mast data have not been adjusted to 10 m as veering is expected to be small.

3.7. Wind Energy Resource Statistics

Wind resource results from the commercial masts cannot be published. Thus only FINO-2 data are available for wind resource comparison in the Baltic Sea study area. Wind speeds are observed at 32, 42, 52, 62, 72, 82, 92, and 102 m. The Wind Atlas Analysis and Application Program (WAsP) [30] has been used to fit the Weibull A and k parameters. To what extent the wind resource at 10 m was estimated similarly from data at all heights was investigated and the result showed variations indicating flow distortion, in particular, at the lower heights. The final result for comparing SAR-based and *in situ* wind resource statistics was estimated from meteorological data at 102 m.

4. Results

4.1. Wind Direction

The comparison results on wind direction are presented first, because these are used to initiate the local wind speed retrieval. The wind directions in the wind maps are the NOGAPS wind directions interpolated in time and space to match locally in each satellite image. Figure 3 shows wind direction from all masts *versus* NOGAPS. In Figure 3 a few observations near 0° and 360° are removed (e.g., in case met-data shows 355° and NOGAPS shows 10°). The data are removed to provide a suitable basis for linear regression within 0–360°. Linear regression results, for each mast for its free stream sector and wake-influenced sector, are listed in Table 3. The statistical results from the free stream sectors and wake-influenced sectors are similar. Therefore the overall result includes all observations, and the overall statistics are given in the last column of Table 3. Figure 4 shows the residual plot.

Figure 3. Wind directions from meteorological stations *versus* NOGAPS, N = 927.

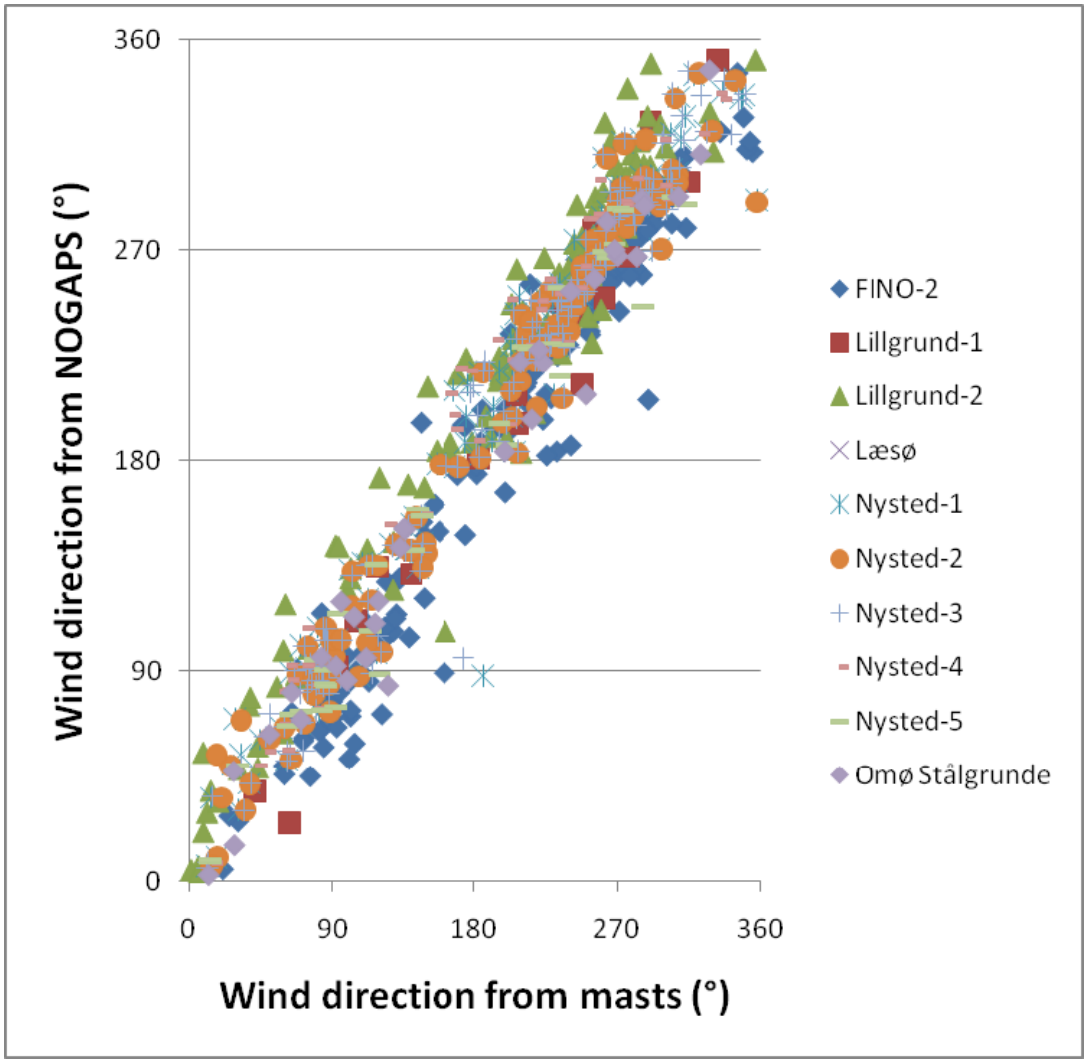

Figure 4. Residual plot for the linear regression on wind direction from masts *versus* NOGAPS.

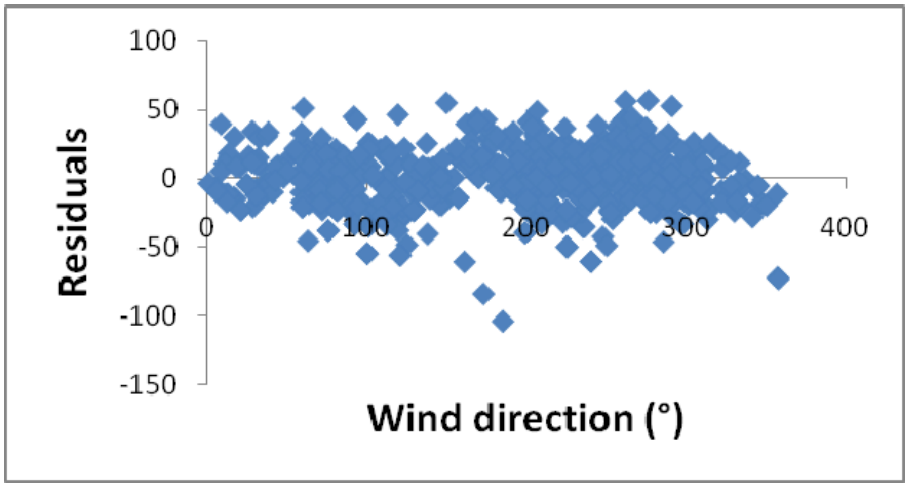

Table 3. Linear regression results for wind direction between masts *versus* NOGAPS in free stream sectors and wake-influenced sectors; and *ALL* includes both free stream and wake-influenced sectors; N is number of samples (−); R^2 is the correlation coefficient(−); SD is standard error (°); RMS is root mean square error (°); bias is the offset of the linear regression (°) and the slope (−).

	FINO2	**Lill.1**	**Lill.2**		**Nys.1**		**Nys.2**		**Nys.3**	**Nys.4**	**Nys.5**	**Omø**	**ALL**
	Free	Free	Free	Wake	Free	Wake	Free	Wake	Free	Free	Wake	Free	**ALL**
N	165	23	77	42	87	47	63	46	155	56	35	35	**927**
R^2	0.952	0.965	0.881	0.971	0.859	0.764	0.805	0.881	0.970	0.970	0.972	0.971	**0.950**
SD	18.95	16.64	16.63	22.67	15.94	19.65	17.51	13.85	15.73	15.70	15.07	16.16	**20.11**
RMS	5.79	4.37	7.86	5.44	8.16	12.68	10.38	6.56	3.85	3.84	3.56	3.88	**6.29**
Bias	−8.44	−11.59	47.16	20.08	48.54	22.71	32.46	12.89	6.83	17.97	5.24	3.02	**7.75**
Slope	1.01	1.05	0.87	1.01	0.86	0.83	0.90	0.93	1.01	1.00	0.97	0.98	**0.99**

4.2. Wind Speed

The comparison results on wind speed are calculated for each meteorological mast taking into account free stream and wind farm wake sectors. The wind directions are taken from NOGAPS to discriminate which directional sector any given pair of wind speeds from a meteorological mast and a SAR wind speed map belongs to. There are more data pairs included in the wind speed analysis than in the wind direction analysis above. Comparison of wind speeds are done also for wind speeds less than 3 m s^{-1} (in contrast to the wind directional comparison analysis) but for winds less than 2 m s^{-1}, the software excludes the SAR-wind data. SAR wind maps contain observations below 2 m s^{-1}, yet the quality of wind speed at this low end is questionable. The linear regression statistics for wind speeds are shown in Table 4(a,b), for free stream sectors and wake sectors, respectively.

The overall correlation coefficient is higher for the free stream sectors (R^2 = 0.783) than for the wake sectors (R^2 = 0.676). In the free stream sectors, the bias is (slightly) negative for all masts except Omø Stålgrunde, whereas it is positive for the wake sectors of Lillgrund-2 and Nysted-1/-2 but surprisingly not for Nysted-5. Positive bias indicates strong microwave returns in the footprint from the wind turbines in the wake sectors.

The turbine affected data are not included in the plot between mast wind speed and SAR-based wind speed shown in Figure 5 and winds less than 2 m s^{-1} in the SAR-wind maps are excluded. The residual plot in Figure 6 shows this omission. Other than that non-linear features do not show and the assumption of a linear fit holds.

Table 4(a) shows that regression using N = 875 samples of collocated wind speed observed at masts and SAR-based wind speed results in R^2 = 0.783, SD = 1.88 m s^{-1} and RMS = 1.17 m s^{-1}. The linear regression slope is 0.96 (with SD = 0.017) and bias −0.25 m s^{-1} (with SD = 0.152 m s^{-1}).

Figure 5. Wind speeds from ten meteorological stations *versus* SAR-based winds, excluding the wake sectors for Lillgrund-2 and Nysted-1/-2/-5, N = 875.

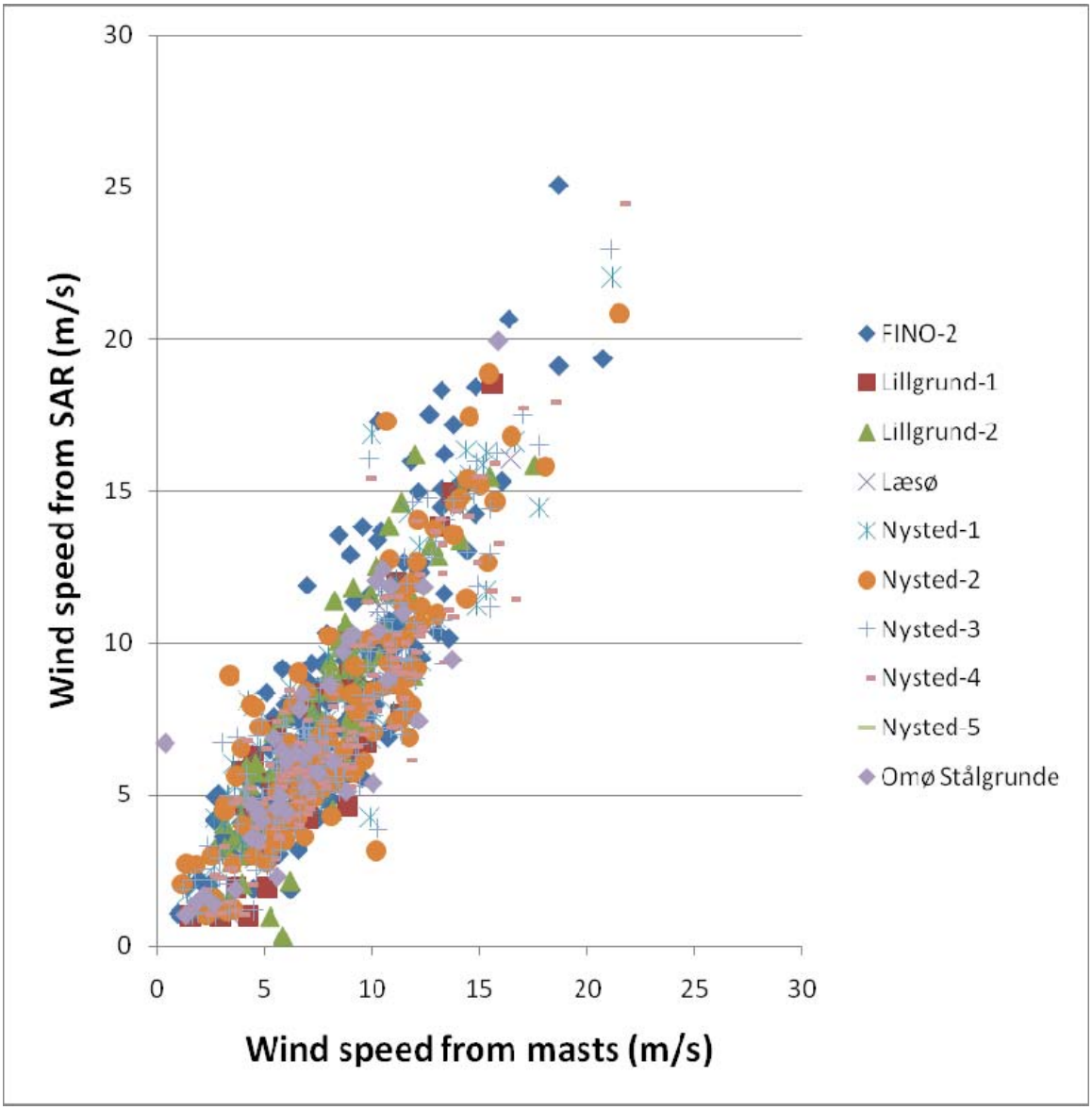

Figure 6. Residual plot for the linear regression on wind speed from masts *versus* SAR wind maps.

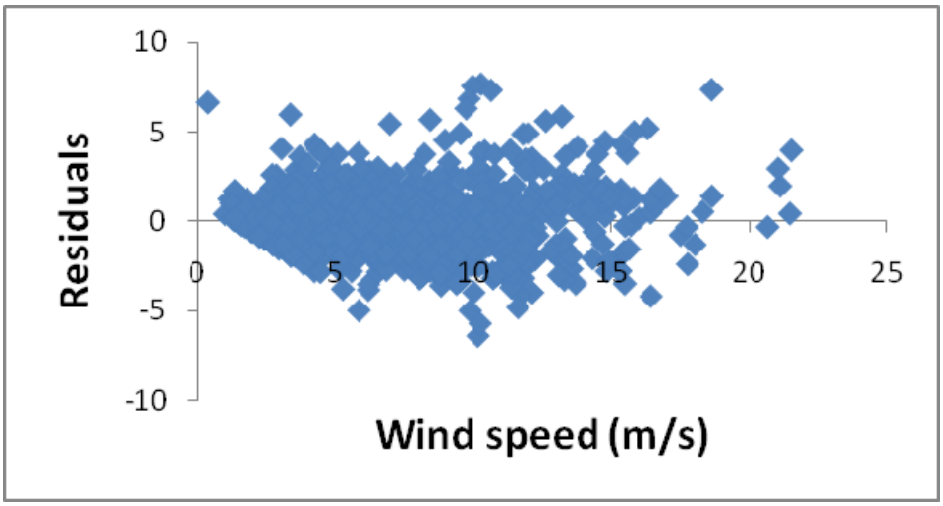

Table 4. **(a)** Linear regression results for wind speed between mast data *versus* SAR-wind maps in **free** stream sectors; **(b)** wake sectors. N is number of samples (−); R^2 is the correlation coefficient (−); SD is standard error (m s^{-1}); RMS is root mean square error (m s^{-1}); bias is the offset of the linear regression (m s^{-1}) and the slope (−).

(a)	**FINO-2**	**Lill.1**	**Lill.2**	**Læsø**	**Nys.1**	**Nys.2**	**Nys.3**	**Nys.4**	**Omø**	**ALL**
N	180	32	86	5	105	110	178	137	42	875
R^2	0.765	0.796	0.789	0.973	0.801	0.754	0.804	0.838	0.686	0.783
SD	2.04	1.90	1.71	1.00	1.88	2.09	1.66	1.62	2.12	1.88
RMS	1.31	1.15	1.05	0.23	1.13	1.37	0.99	0.89	1.55	1.17
Bias	−0.21	−1.34	−0.61	−2.32	−0.06	−0.10	−0.22	−0.45	0.22	−0.25
Slope	1.03	1.08	1.06	1.16	0.93	0.92	0.92	0.95	0.92	0.96

(b)	**Lill.2**	**Nys.1**	**Nys.2**	**Nys.4**	**ALL**
N	51	65	57	41	214
R^2	0.719	0.669	0.686	0.740	0.676
SD	1.89	1.59	1.58	2.04	1.85
RMS	1.31	1.19	1.15	1.37	1.36
Bias	0.52	0.94	0.98	-0.78	0.57
Slope	1.06	0.80	0.82	1.03	0.91

4.3. Wind Resource Statistics

The wind energy resource statistics in the Baltic Sea study area are calculated based on 1009 Envisat ASAR wind maps using the method in [8] with equal weights to all. The data represent seasons and twice-daily conditions (*cf.* Table 1).

The resulting SAR-based maps at 1 km by 1 km resolution are presented in Figure 7(a–d). The first panel in Figure 7 shows the number of samples and the following three panels show SAR-based results on Weibull A and k, and wind power density, E. The map of overlapping samples shows the

characteristic pattern of satellite passes inclined from ascending and descending tracks. There are more samples in the northwest part of the study area and less in the southern region. The maximum number of samples is 538 and the minimum number around 350. Weibull A ranges from 6 m s^{-1} along the eastern Swedish coast to 9.5 m s^{-1} in the Skagerrak Strait, and Weibull k ranges from 1.4 near coastlines up to 2.1 in the southwestern part of the study area. In Figure 7(b,c) too high values are found at the Nysted (Rødsand 1) wind farm due to backscatter from the 72 turbines. Wind power density values range from 249 W m^{-2} to 934 W m^{-2}. The highest wind power density value is found in the Skagerrak Strait, not in the Baltic Sea.

Figure 7. Wind resource statistics based on 1009 Envisat ASAR wide swath mode satellite wind maps covering part of the Baltic Sea and interior Danish Seas. Panels top: **(a)** number of samples (−); **(b)** Weibull A (m s^{-1}); **(c)** Weibull k (−); and **(d)** wind power density (W m^{-2}) including indication of wind farms. The wind farm numbers refer to Appendix 1.

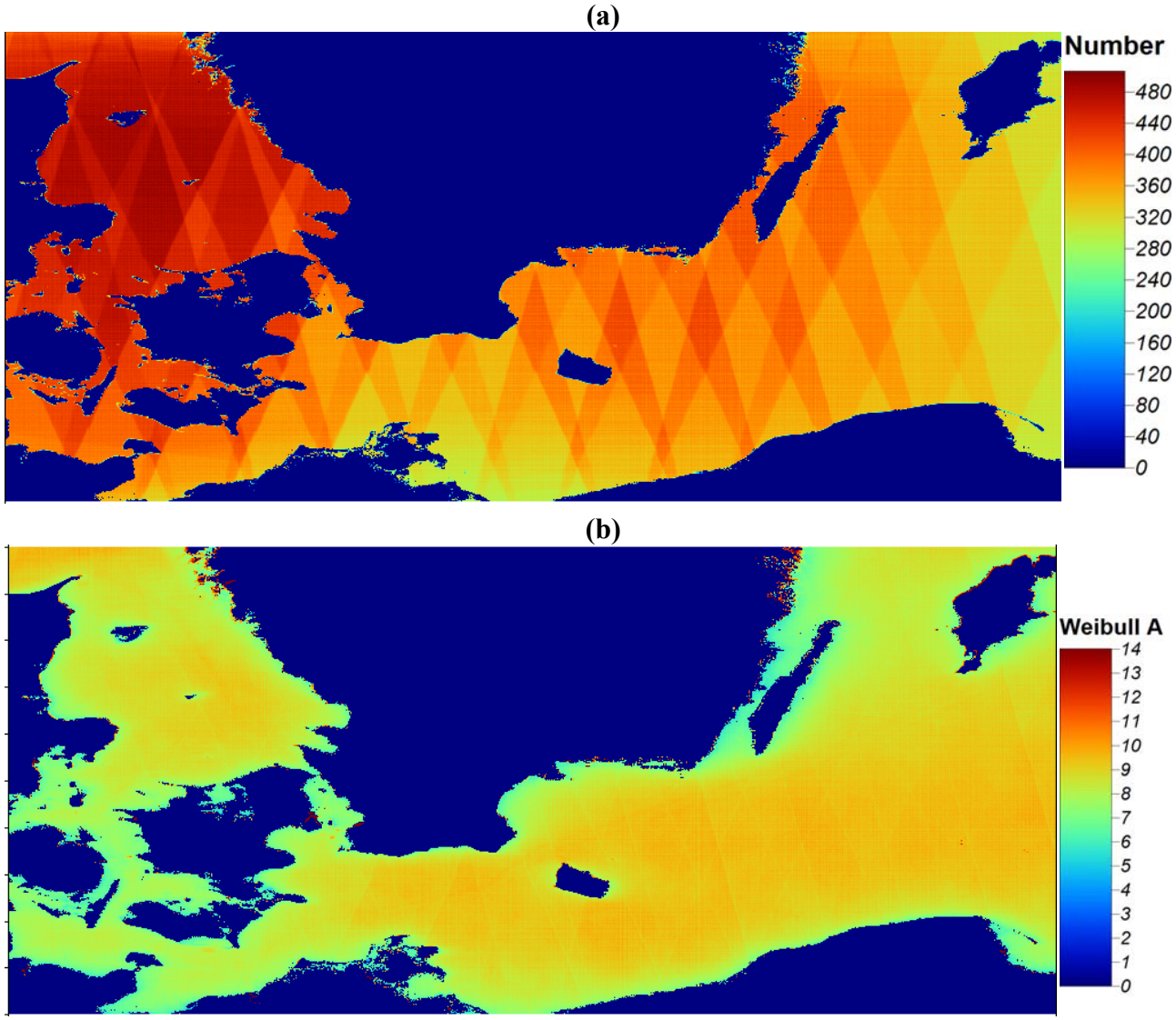

Figure 7. *Cont.*

(c)

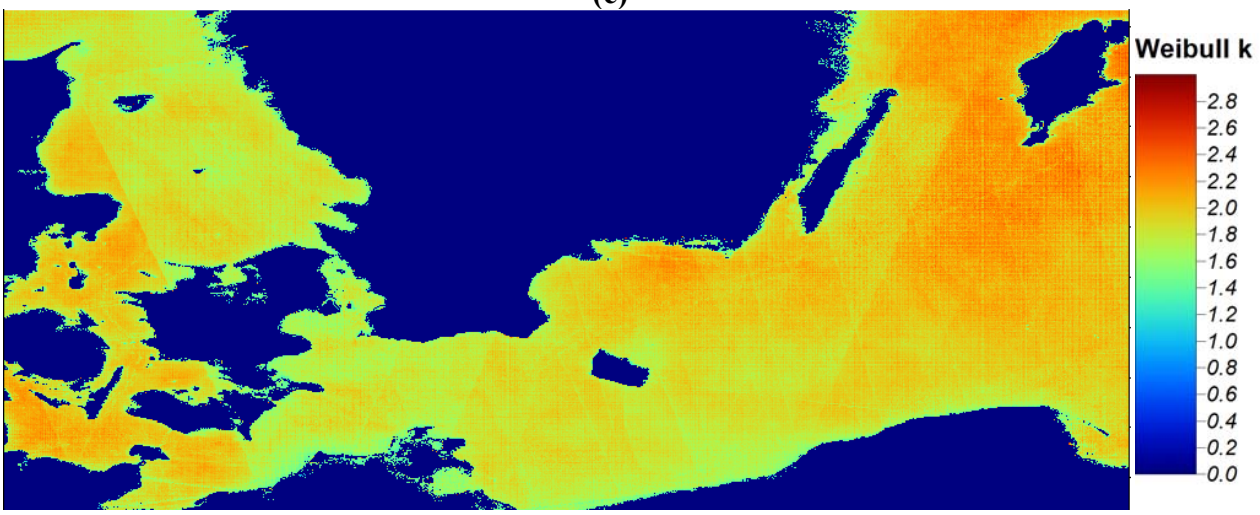

(d)

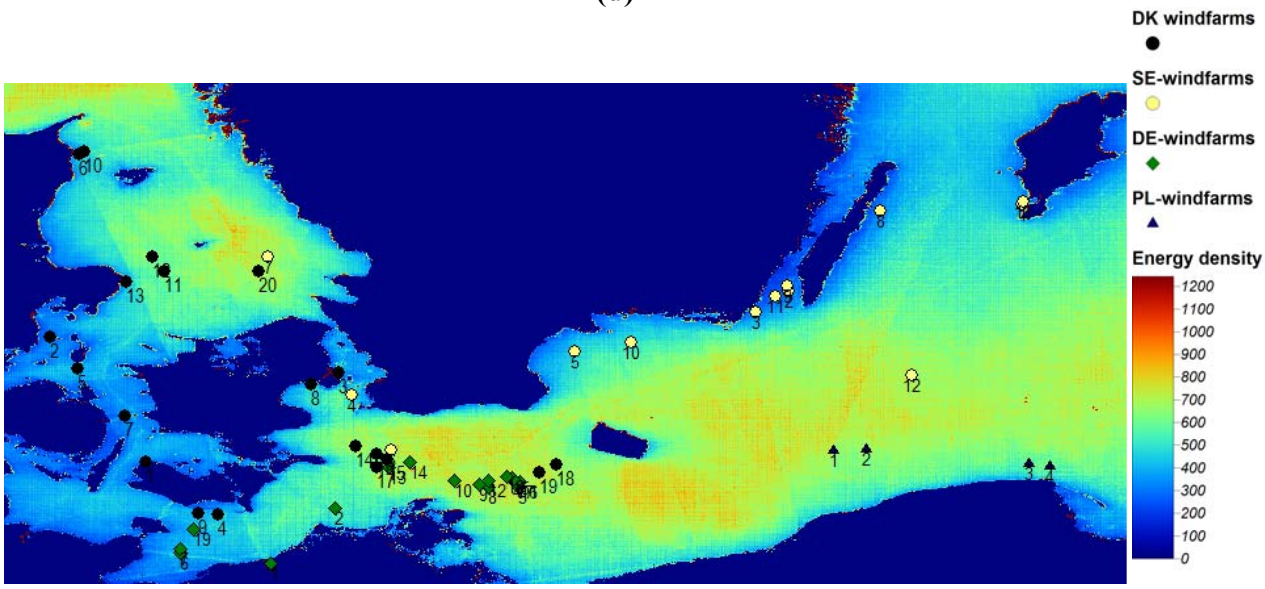

Comparison of the SAR-based wind resource statistics is done for FINO-2. Firstly though, the FINO-2 data observed at eight levels during three years from 1 August 2007 to 31 July 2010 are shown in Figure 8 including the logarithmic profiles for all. Observations at the lower heights appear to be flow distorted (reduced) and none of the other data fall onto one profile. The 102 m data appear not to be reduced and are used to estimate the wind resource at 10 m using data from 9 December 2007 to present. The SAR wind maps are from 2003 to 2010.

The wind speed distribution at FINO-2 and the SAR-based data are shown in a histogram in Figure 9 and wind resource results are listed in Table 5. The SAR-based result appears to estimate mean wind speed and Weibull A well, but over-predicts the wind power density by 29%.

Figure 8. FINO-2 mean wind speed at eight levels observed from 1 August, 2007 to 31 July 2010 using 89,394 concurrent samples and logarithmic profiles extrapolated to 10 m from each of the eight observation heights.

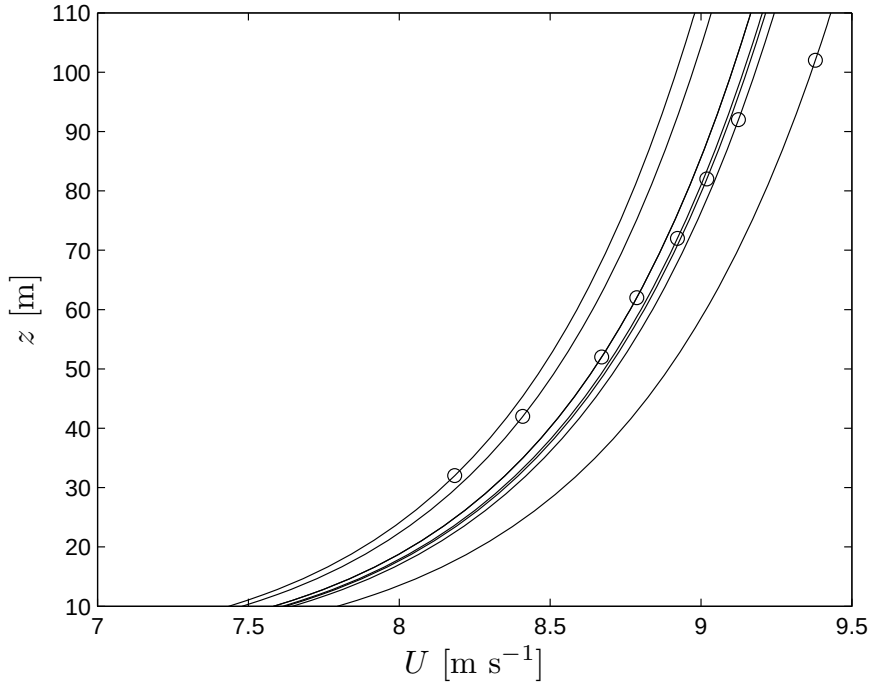

Figure 9. Histogram of wind speed observed at FINO-2 extrapolated from 102 m to 10 m from 1 July 2007 to 19 October 2010 total of 146,910 samples (in grey) with Weibull fit using WAsP, and wind speed observed from Envisat ASAR from 2003 to 2010, total of 409 samples (in black) with Weibull fit using WAsP.

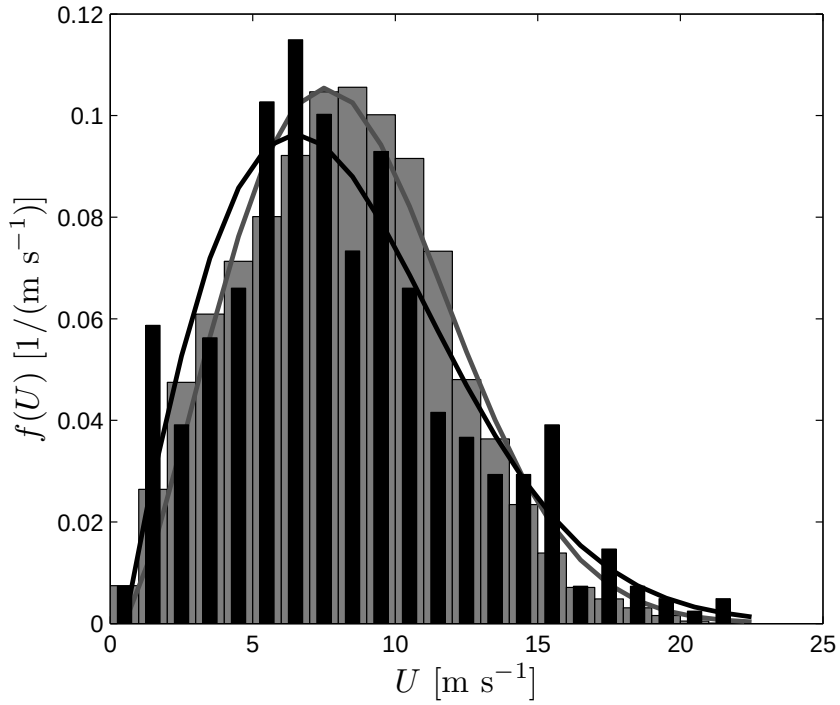

Table 5. Wind resource statistics at FINO-2 using all meteorological observations at 102 m extrapolated to 10 m using WasP. For SAR wind maps using WAsP and using maximum likelihood (M.L.) and the differences SAR normalized with mast data (in percentage).

FINO-2	Mast (WAsP)	SAR (WAsP)	SAR (M.L.)	Difference (%) (WAsP-WAsP)	Difference (%) (WAsP-M.L.)
Mean wind speed (m s^{-1})	8.12	8.17	8.16	0.5	0.6
Weibull A (m s^{-1})	9.00	8.72	9.21	2.3	3.1
Weibull k (−)	2.31	1.94	1.93	−16.9	−16.0
Power density (W m^{-2})	521	559	670	7.3	28.6
N (-)	146,910	409	409	-	-

The SAR-based mean wind speed, A, k and E at the position of the 17 meteorological masts are listed in Table 6. The mean wind speed tends to increase with distance from the nearest coastline as graphed in Figure 10. It should be noted that the effect of nearby wind turbines is neglected. For certain sites and wind directions too high wind speed values may occur due to backscatter from the turbines, but may also include wind farm wake areas with reduced wind speed. For Midgrund the distance to the nearest wind turbines is ~600 m, islands or ships may explain this too high value. Thus the results for the sites with nearby wind turbines are clearly not valid for free stream wind resource assessment.

Table 6. SAR-based wind resource statistics listed with increasing mean wind speed (U), and including wind power density (E), Weibull A and k, number of samples (N) and the distance to the nearest coast. The satellite wind maps are from Envisat ASAR from March 2003 to April 2010. Sampling uncertainties are shown in brackets. *nearby wind farm.

Met-station	U (m s^{-1})	E (W m^{-2})	A (m s^{-1})	k (−)	N (−)	Dist. (km)
Vindeby SMS*	6.67 (±0.16)	346(±24)	7.53 (±0.18)	2.04 (±0.07)	463	0.3
Vindeby SMW*	6.74 (±0.20)	459(±40)	7.53 (±0.23)	1.63 (±0.05)	468	1.7
Omø Stålgrunde	6.90 (±0.16)	364 (±24)	7.79 (±0.18)	2.16 (±0.08)	464	10.4
Sky2000	7.01 (±0.18)	401 (±29)	7.92 (±0.20)	2.05 (±0.08)	417	14.7
Lillgrund-2*	7.18 (±0.20)	477(±39)	8.09 (±0.23)	1.85 (±0.07)	418	8.7
Lillgrund-1*	7.22 (±0.20)	483(±39)	8.14 (±0.23)	1.86 (±0.07)	415	8.7
Gedser Rev	7.22 (±0.20)	498(±42)	8.12 (±0.23)	1.81 (±0.07)	423	9.5
Nysted-3*	7.29 (±0.18)	446(±32)	8.23 (±0.20)	2.07 (±0.08)	439	9.2
Nysted-4*	7.30 (±0.18)	451(±32)	8.24 (±0.20)	2.05 (±0.07)	441	6.9
Nysted-1*	7.37 (±0.18)	453(±31)	8.32 (±0.20)	2.11 (±0.08)	438	7.1
Nysted-2*	7.45(±0.17)	460(±31)	8.41 (±0.20)	2.14 (±0.08)	439	7.3
Nysted-5*	7.70 (±0.18)	500(±33)	8.69 (±0.20)	2.18 (±0.08)	438	11.8
Læsø	7.70 (±0.19)	593(±42)	8.67 (±0.21)	1.84 (±0.06)	540	13.9
Midgrund*	7.90 (±0.25)	777(±75)	8.80 (±0.29)	1.58 (±0.05)	424	2.3
Stora Middelgr.	7.99 (±0.19)	618 (±42)	9.01 (±0.21)	1.96 (±0.07)	525	29.7
FINO-2	8.16 (±0.22)	670(±53)	9.21 (±0.25)	1.93 (±0.07)	409	38.2
Arkona-Becken-S.	8.17 (±0.23)	714(±60)	9.19 (±0.26)	1.83 (±0.07)	407	37.1

Figure 10. SAR-based mean wind speed (top) and wind power density (bottom) at the location of 17 meteorological masts, near or far from wind farms.

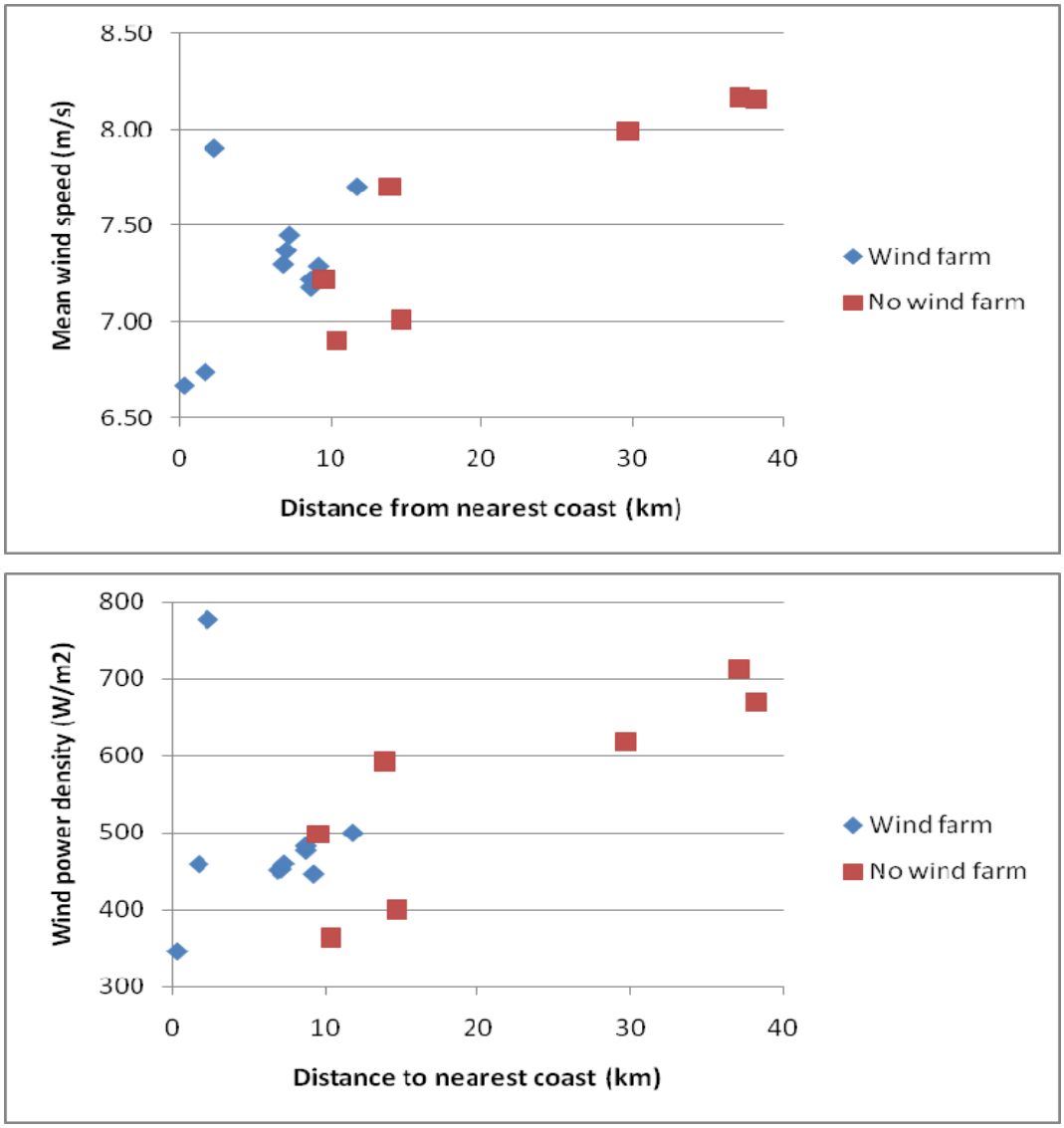

Finally, the wind resource statistics based on satellite SAR wind maps are calculated for existing and planned offshore wind farms in the study area. The existing wind farms include nine in Denmark, four in Sweden and one in Germany. The three largest are Rødsand 2 with 90 turbines and a total of 207 MW installed capacity since August 2010; Rødsand 1 with 72 turbines and a total of 166 MW installed capacity since 2003; and Lillgrund with 48 turbines and a total of 110 MW installed capacity since 2007.

There are plans of adding 42 new wind farms in the study area in coming years. A list of existing and planned wind farms is provided in Appendix A. The information on the wind farms is taken mainly from http://www.4coffshore.com/windfarms. The wind resource statistics for existing and planned wind farms are calculated based on SAR wind maps. The results include mean wind speed, Weibull A and k, wind power density and the number of wind maps used at each wind farm. Figure 11 shows mean wind speed per country, and Figure 12 shows Weibull A and k, and wind power density as a function of distance to the nearest coastline.

Figure 11. Mean wind speed from Envisat ASAR observations at existing and planned wind farm sites per country in the Baltic Sea study area (*cf.* Table A1).

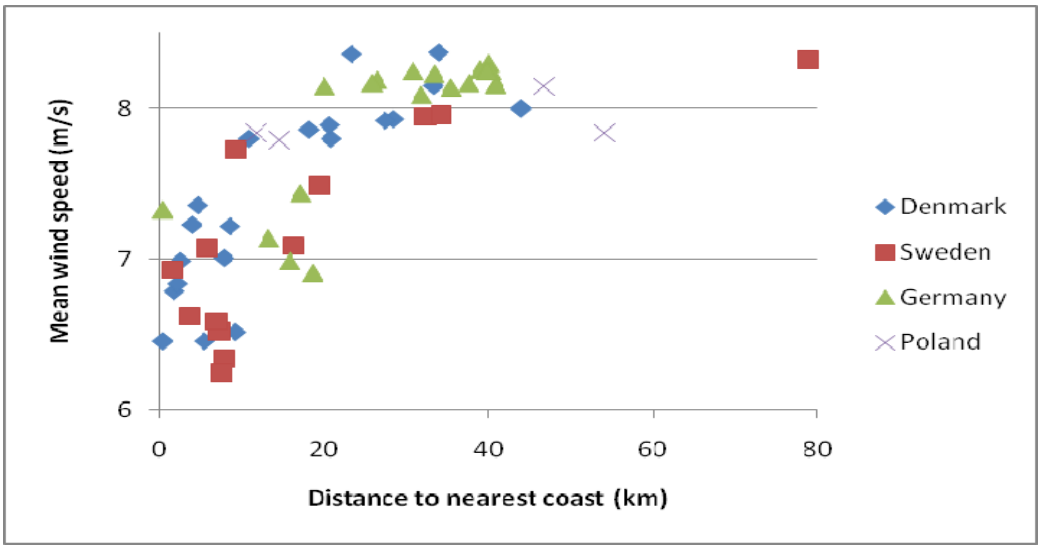

Figure 12. Weibull A and k (top) and wind power density (bottom) calculated from Envisat ASAR observations at existing and planned wind farms in the study area.

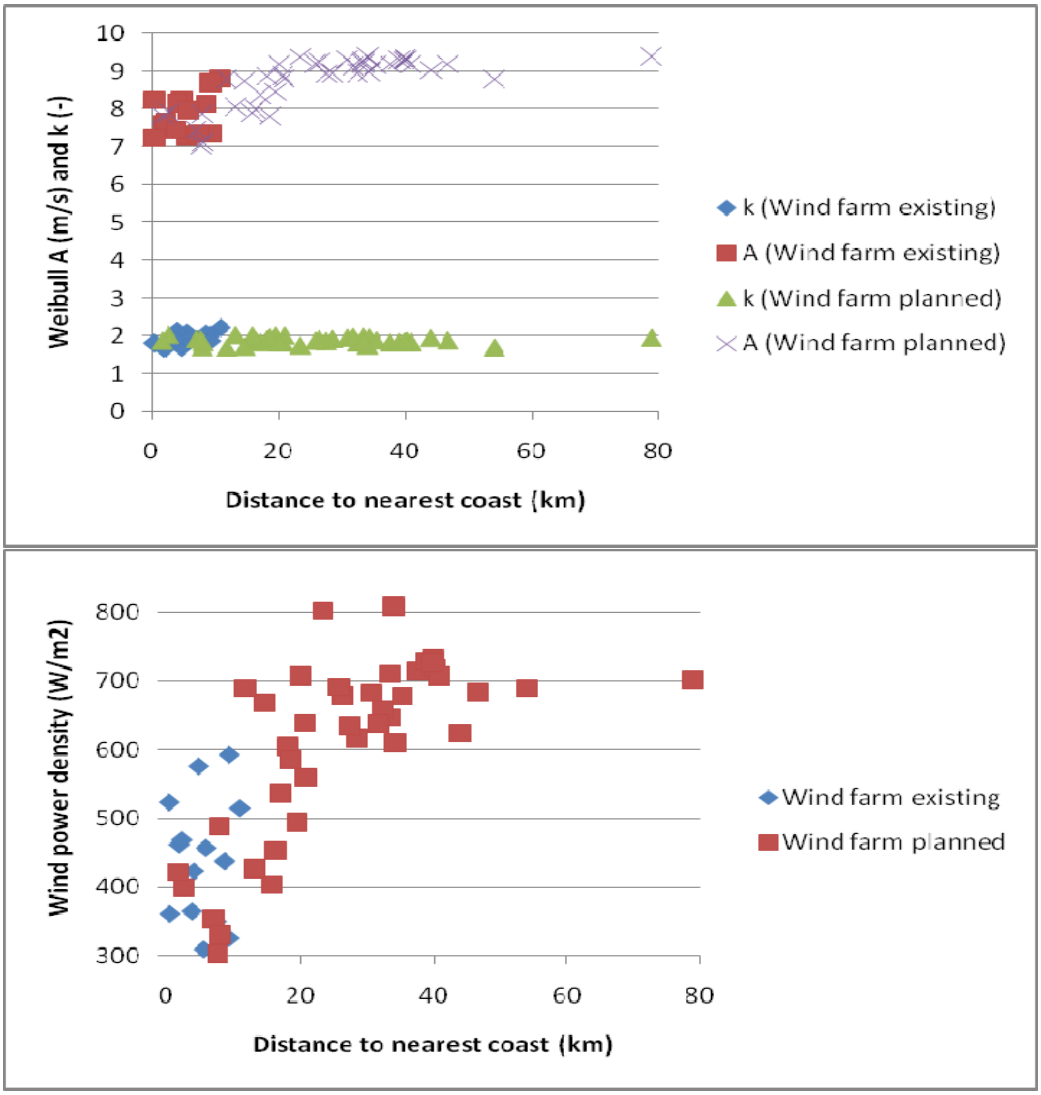

5. Discussion

5.1. Wind Direction Comparison

The comparison results between NOGAPS wind direction and meteorological observations are highly correlated with R^2 of 0.950 and RMS at 6.29°. The linear regression slope is 0.99 and the bias 7.75° (*i.e.*, ~2%). Around 900 independent samples are used. The clockwise veering is partly explained by the Ekman spiral that veers clockwise in the northern hemisphere. The overall wind direction statistics show good accuracy.

The reproducibility, *i.e.*, the variation arising using the same method among different met-stations, is very good. Very few extreme outliers in the NOGAPS wind directions are found. Systematic problems do not appear at the investigated locations. Studies have shown that wind direction may be obtained from the SAR image itself by identification of the wind streaks aligned approximately with the dominant wind direction, e.g., [31]. The optimal situation is to use directions from streaks, yet problems associated with automatic streak detection limits this option. Further, it has been shown that using wind direction from a local mast to initiate the local wind retrieval also provides very good results locally [8]. Only very few meteorological masts are available and, for near-real-time SAR wind mapping, this is not a viable option. However, it can be done offline as post-processing for a specific local site in order to increase the accuracy nearby. It has to be kept in mind though that wind directions are neither constant in time nor in space. It is clear that mesoscale atmospheric phenomena occur in this enclosed sea with many islands, see Figure 2. But despite this fact, the NOGAPS global model appears to provide good wind directions. This is important as the wind speed retrieval is initiated with the NOGAPS wind directions.

5.2. Wind Speed Comparison

The overall statistics from the wind speed regression analysis are also of good quality, though with lower R^2 than for wind directions. It is the first time that a comprehensive data set of high-quality meteorological masts—all designed for wind resource assessment—has been used for comparison to SAR-based winds. For five masts more than 100 collocated pairs are available. The wind speed statistics based on nearly 900 collocated pairs of meteorological observations from a total of ten masts and SAR-based winds in free stream (not including noise from wind turbine backscatter) show R^2 0.783, SD 1.88 m s^{-1} and RMS 1.17 m s^{-1}. There is a small negative bias −0.25 m s^{-1} (with SD 0.152 m s^{-1}) and the linear regression slope is 0.960 (with SD 0.017). The statistics are comparable to results from Horns Rev in the North Sea [8,22] and clearly better than the nominal accuracy of the geophysical model function with ±2 m s^{-1} accuracy [17,32]. The water depth at FINO-2 is 25 m whereas it ranges from 4 to 10 m at Lillgrund and from 6 to 10 m at Læsø, Nysted and Omå Stålgrunde. Tidal currents are insignificant, thus effects of SAR signatures originating from currents are expected to be small. Averaging to 1 km by 1 km grid suppresses small-scale effects.

5.3. Wind Resource Comparison

In the Baltic Sea study area only wind resource statistics from FINO-2 are available for comparison with results from SAR. The results show near zero difference between mean wind speed from mast data and SAR using an extrapolation of wind speed data from 102 m to 10 m. Further the result deviates ~2% on Weibull A but ~16 % on Weibull k. It is statistically more difficult to estimate the Weibull k parameter than the Weibull A parameter. More data are needed to achieve similar accuracy. According to [25] it is necessary with ~70 samples to estimate Weibull A, ~175 samples to estimate Weibull k, and ~2,000 samples to estimate power density within ±10% accuracy at the 90% confidence interval. At FINO-2 the difference in power density values is ~29% using 409 samples comparing results from mast data observed at 102 m using maximum likelihood for Weibull fitting. Using WAsP Weibull fitting to the SAR data (shown in Figure 9 and listed in Table 5) the difference in power density is ~7% between mast data and SAR.

The uncertainty on maximum likelihood fitting is listed in Table 6 and typically is within 50 W m^{-2}. The choice of Weibull fitting influence results as seen in Table 5. Unfortunately only one location is available for comparison of wind energy density results. The FINO-2 meteorological data shown in Figure 8 shows a tendency to have (much) higher winds high in the atmosphere than the logarithmic profile. This may be caused either by: (1) Flow distortion at lower observational heights; (2) stable stratification; or (3) coastal winds that are not fully adjusted [33]; or a combination of the all three.

The vertical extrapolation adds uncertainty. The wind speed data appear to be influenced by the relatively heavy mast construction that is likely to add flow distortion to the wind measurements. It was found that the collocated wind speeds at FINO-2 are less well correlated than for most other masts, see Table 4. No further assessment has been made. Recent results from the North Sea [10] comparing mean wind speed, Weibull A and k, and power density between three masts (Horns Rev, Høvsøre and FINO-1) and SAR-based results have shown deviations less than 5% for mean wind speed and Weibull A and deviations less than 7% for Weibull k and power density, using approximately the same number of SAR samples. Reasons for the better agreement in the North Sea compared to the Baltic Sea could be differences in atmospheric stability. The more enclosed Baltic Sea, where the coastal flow may not be fully adjusted, could be another reason [33].

Weibull statistics are published from three masts in the study area based on meteorological data observed ~50 m above sea level in the 1990'ties, *i.e.*, prior to Envisat. The published results are Weibull A and k of 9.1 m s^{-1} and 2.3 at 48 m height observed from 1993 to 1997 at Vindeby [34], Weibull A and k of 8.3 m s^{-1} and 2.3 at 50 m observed from October 1997 to July 1998 at Midgrund [35], and Weibull A and k of 8.6 m s^{-1} and 2.65 observed at 50 m from March to November 1999 at Omø Stålgrunde [36]. For two masts the data cover less than one year. At Midgrund and Vindeby wind turbines influence the atmospheric flow and the SAR-based results do not reflect free flow conditions. Comparisons are not attempted due to these conditions.

5.4. Examination of Wind Resource Statistics

Examination of the SAR-based maps of Weibull A, k and wind power density (Figure 7) shows as expected higher wind power density value in relatively open seas. The lee effect of islands in the Kattegat Strait and Baltic Sea are notable with lower wind power density value near the islands. The offshore wind climate in the Danish interior seas has lower wind power density than Kattegat, Skagerrak and most of the Baltic Sea. It is noted that Weibull k appears to be higher in the southwestern part of the study area than elsewhere. High k indicates relatively steady winds.

The wind resource statistics presented for the 17 meteorological masts (Table 6, Figure 7) show a trend of higher mean wind speed further offshore. The mean wind speed ranges from 6.7 m s^{-1} to 8.2 m s^{-1} with an uncertainty of ±0.2 m s^{-1}. The masts are located from the coast to ~40 km offshore. Midgrund is seen as an outlier with much higher mean wind speed, Weibull A and wind power density than other masts at similar distance to the coast. The high values at Midgrund are most likely due to two wind turbines located less than 600 m from the mast position, nearby islands and ships giving very high backscatter and therefore unrealistically high winds.

Reflection from turbines alters backscatter values. It is seen at the Nysted-1 wind farm (Figure 7(b–d). This wind farm has existed since 2003. Also the Lillgrund can be seen. Lillgrund has operated since 2007 whereas Rødsand-2 (from 2010) cannot be clearly seen in the maps.

The SAR-based mean wind speed, Weibull A and wind power density at the Vindeby, Lillgrund and Nysted masts appear not to be notably affected by wind turbine reflections in contrast to the Midgrund mast. This is concluded as the wind statistics at Vindeby, Lillgrund and Nysted increase gradually with distance from the coast and also compare well with similar statistics from masts not affected by wind turbines (Figure 8).

The Nysted-3/-4 masts are not affected by turbine backscatter but both are affected by wake for westerly winds, thus the results are expected to be (slightly) negatively biased compared to the condition prior to the wind farm. Wind farm wake deficit, *i.e.*, reduced wind downwind of a wind farm, typically is of the order ~10% but may vary dependent upon turbine operations, wind speed and atmospheric static stability. For more detail on SAR-based wake mapping see [11,37].

It is remarkable how low winds are observed by SAR for Omø Stålgrunde and Sky2000. Both have mean wind speed of ~7.0 m s^{-1} whereas Læsø also located ~12 km offshore shows a mean wind speed of ~7.7 m s^{-1} (see Table 6). Near Læsø, Omø Stålgrunde and Sky2000 there are no wind farms or other obstacles and the major difference between these three masts is the more open sea at Læsø (Figures 1 and 7). In Figure 7(d), the energy density map shows high values in the Great Belt between Zealand and Fyn along the Great Belt Bridge. More interestingly, an S-shape curve east of the Sprogø windfarm identical to the major ship route for large vessels shows clearly. This is probably due to reflection from ships.

The mean wind speed at existing and planned wind farm locations in the four countries (Table A1, Figure 11) shows a gradual increase as a function of further distances to the nearest coast. There is a significant variation (±0.7 m s^{-1}) in the coastal zone from 0 to 20 km offshore with a mean wind speed ~7.0 m s^{-1}. Beyond 20 km offshore the mean wind speed is ~8.1 m s^{-1} and varies only ±0.2 m s^{-1} in all four countries, Denmark, Germany, Poland and Sweden. Increases in coastal winds previously has been studied with similar results [33].

Further details on the SAR-based wind resource statistics are shown in Figure 10 with the Weibull A and k and wind power density results with marking of existing and planned wind farms. It is noticed that all existing wind farms are located less than 11 km offshore whereas only a few new wind farms are planned this close to land. Many wind farms are planned in the 15 to 20 km zone and wind power density is seen to vary from 400 to 700 W m^{-2}. The two extremes are Beta Baltic and Arcadis Ost1, see Table A1. In the coastal zone from 20 km and further offshore, out to 80 km with the Swedish Södra Midsjöbanken as frontier very far offshore, the wind power density tends to range between 600 and 720 W m^{-2} with two outliers above, namely Rønne Banke X and V with 800 W m^{-2}.

The statistical uncertainty on mean wind speed is ~2 to 3% when based on roughly 400 samples and similar for Weibull A. The uncertainty on wind power density is much higher ~7 to 9% and similar for Weibull k for a data set of this size. According to [25], Weibull A and k may be estimated with ±10% accuracy and 90% confidence using ~75 and ~175 samples, respectively (assuming perfect data).

The present data set represents all seasons and morning and evening conditions. The SAR coverage is not homogeneous (Figure 7(a)) and it reflects in results of Weibull k and energy density in Denmark (a northwest–southeast line) and in the Baltic Sea (a northeast–southwest line). The reason could be few particular images giving strong impact.

For Breitling only 161 valid samples are found which is due to the location. Breitling is located in an enclosed harbor area in Rostock, not truly offshore, and therefore the footprint often includes land and the values are discarded from the series. Furthermore, ocean wind mapping is not adequate in enclosed water but the wind statistics, surprisingly enough, falls nicely within the other results.

The number of samples is important as well as how well the samples represent the general wind climate as described in [10]. The variation in wind speed during the day is not resolved by SAR-based wind maps as these are observed either in the morning or evening passes according to the orbital parameters. Thus diurnal variation in wind speed may add uncertainty. Seasonal wind variations may add uncertainty in case the wind maps do not cover the full year as would be the case, for example, in cold climate regions with sea ice during winter.

SAR-based results are valid at 10 m. A challenging issue is the vertical extrapolation of the SAR-based wind results up to hub-height. The wind data from FINO-2 indicate the problem. Present and future wind turbines may operate at 100 m to 300 m above sea level. In the EU-Norsewind project the vertical extrapolation is being investigated using data from an array of wind profiling lidars observing at 70 to 200 m above sea level installed in the Northern European Seas. Lidar-based results show that the wind profile deviates from the surface-layer wind profile high in the boundary layer [38-41]. Mesoscale modeling of the offshore wind resource is on-going and comparison of results is in progress, yet beyond the scope of the present paper.

The present analysis is based on Envisat ASAR images. More Envisat ASAR images could be extracted from the archive as well as imagery from ERS-1/-2, Radarsat-1/-2 and ALOS PALSAR. The study, however, is the most comprehensive of its kind on wind resource mapping of the Baltic Sea area.

6. Conclusions

The study presents SAR-based ocean winds compared to wind observations from 10 meteorological masts erected specifically for wind energy mapping in part of the Baltic Sea. Around 900 collocated

pairs of Envisat ASAR wide swath mode images and *in situ* data, show the wind speed to be mapped with root mean square error 1.17 m s^{-1}, bias −0.25 m s^{-1}, standard deviation 1.88 m s^{-1}, and correlation coefficient R^2 of 0.783. Ocean wind is mapped from CMOD-5, using wind direction input from a global atmospheric model, and comparison results on wind direction between the model and *in situ* data are root mean square error 6.29°, bias 7.75°, standard deviation 20.11°, and R^2 of 0.950. Using more than 1000 Envisat ASAR wind maps, SAR-based wind resource statistics are examined for the 12 existing and 42 planned wind farms in the study area. It is found that the variation in mean wind is highly variable in the near coastal zone from 0 to 20 km. All existing wind farms are located less than 11 km from the nearest coast but most of the planned wind farms will be located further offshore. Here the SAR-based results indicate high mean wind speed and high wind power density. It is noted that the wind power density ranges from 300 to 800 W m^{-2} for the planned wind farms. Wind resource statistics are compared only at one meteorological mast, FINO-2, showing Weibull A to deviate ~2% between *in situ* and SAR-based results, but Weibull k to deviate ~16%. The power density is found to deviate ~29% which is considerably higher than found in a recent study in the North Sea using *in situ* data from three masts. In the North Sea, the deviations between masts data and SAR-based results were within 7% on Weibull k and power density using approximately a similar number of samples and similar wind retrieval. Further investigation on vertical extrapolation is needed.

Acknowledgements

The work was supported by the EU-Norsewind project (TREN-FP7EN-21908) and the EU-South Baltic OFF.E.R (EU European Development Fund and the South Baltic Program). Satellite data are provided by the European Space Agency (Cat. 1 project 3644 and ESA-CSA SOAR project 6773). Meteorological data from DONG Energy from Nysted, Omø Stålgrunde and Læsø masts as well as meteorological data from Vattenfall from the Lillgrund masts are greatly acknowledged. Also FINO-2 meteorological data from the Forschungsplattformen in Nord- und Ostsee from Bundesamt für Seeschifffahrt und Hydrographie (BSH) are greatly acknowledged. The Johns Hopkins University, Applied Physics Laboratory, USA is thanked for providing and supporting the APL/NOAA SAR Wind Retrieval System (ANSWRS).

References

1. Horstmann, J.; Koch, W.; Lehner, S. Ocean wind fields retrieved from the advanced synthetic aperture radar aboard ENVISAT. *Ocean Dyn.* **2004**, *54*, 570-576.
2. Monaldo, F.M.; Thompson, D.R.; Winstead, N.S.; Pichel, W.G.; Clemente-Colón, P.; Christiansen, M.B. Ocean wind field mapping from synthetic aperture radar and its application to research and applied problems. *Johns Hopkins Apl. Tech. Dig.* **2005**, *26*, 102-113.
3. Kerbaol, V. Near-Real Time Generation of ENVISAT ASAR Level-2 Wind and Waves Products: Presentation of the System and Preliminary Achievements. In *Proceedings of SEASAR 2008—2nd International Workshop on Advances on SAR Oceanography from ENVISAT and ERS Missions*, Rome, Italy, January 21–25, 2008; ESA: Paris, France, 2008.

4. Kerbaol, V. Improved Bayesian Wind Vector Retrieval Scheme Using ENVISAT ASAR Data: Principles and Validation Results. In *Proceedings of ENVISAT Symposium 2007*, Montreux, Switzerland, April 23–27, 2007; ESA-SP-636; European Space Agency: Paris, France, 2007.
5. Monaldo, F.; Kerbaol, V.; Clemente-Colón, P.; Furevik, B.; Horstmann, J.; Johannessen, J.; Li, X.; Pichel, W.; Sikora, T.D.; Thomson, D.J.; Wackerman, C. The SAR Measurement of Ocean surface Winds: An Overview. In *Proceedings of the Second Workshop Coastal and Marine Applications of SAR*, Svalbard, Norway, September 2–12, 2003, ESA: Paris, France, 2003; pp. 15-32.
6. Beal, R.C.; Young, G.S.; Monaldo, F.; Thompson, D.R.; Winstead, N.S.; Schott, C.A. *High Resolution Wind Monitoring with Wide Swath SAR: A User's Guide*; U.S. Department of Commerce: Washington, DC, USA, 2005; pp. 1-155.
7. Johannessen, O.M.; Bjorgo, E. Wind energy mapping of coastal zones by synthetic aperture radar (SAR) for siting potential windmill locations. *Int. J. Remote Sens.* **2000**, *21*, 1781-1786.
8. Christiansen, M.B.; Koch, W.; Horstmann, J.; Hasager, C.B. Wind resource assessment from C-band SAR. *Remote Sens. Environ.* **2006**, *105*, 68-81.
9. Hasager, C.B.; Barthelmie, R.J.; Christiansen, M.B.; Nielsen, M.; Pryor, S.C. Quantifying offshore wind resources from satellite wind maps: Study area the North Sea. *Wind Energy* **2006**, *9*, 63-74.
10. Badger, M.; Badger, J.; Nielsen, M.; Hasager, C.B.; Peña, A. Wind class sampling of satellite SAR imagery for offshore wind resource mapping. *J. Appl. Meteorol. Climatol.* **2010**, (in press).
11. Christiansen, M.B.; Hasager, C.B. Wake effects of large offshore wind farms identified from satellite SAR. *Remote Sens. Environ.* **2005**, *98*, 251-268.
12. Larsén, X.G.; Mann, J.; Berg, J.; Göttel, H.; Daniela, J. Wind climate from the regional climate model REMO. *Wind Energy* **2010**, *13*, 279-298.
13. Larsén, X.G.; LARSEN, S.E.; Badger, M. A case study of mesoscale spectra of wind and temperature, observed and simulated. *Q.J.R.Meteorol. Soc.* 137, DOI: 10.1002/qj.739, **2010**.
14. Horstmann, J.; Koch, W. Evaluation of an Operational SAR Wind Field Retrieval Algorithm for ENVISAT ASAR. In *Proceedings of 2004 IEEE International Geoscience and Remote Sensing Symposium*, Anchorage, AK, USA, September 20–24, 2004.
15. Christiansen, M.B.; Hasager, C.B.; Thompson, D.R.; Monaldo, F. Ocean winds from synthetic aperture radar. In *Ocean Remote Sensing: Recent Techniques and Applications*; Niclos, R., Caselles, V., Eds.; Research Singpost: Kerala, India, 2008; pp. 31-54.
16. Hasager, C.B.; Peña, A.; Christiansen, M.B.; Astrup, P.; Nielsen, M.; Monaldo, F.M.; Thompson, D.R.; Nielsen, P. Remote sensing observation used in offshore wind energy. *IEEE J. Sel. Topics Appl. Earth Obs. Remote Sens.* **2008**, *1*, 67-79.
17. Hersbach, H.; Stoffelen, A.; de Haan, S. An improved C-band scatterometer ocean geophysical model function: CMOD5. *J. Geophys. Res.* **2007**, *112*, C03006.
18. Monaldo, F.M.; Thompson, D.R.; Beal, R.C.; Pichel, W.G.; Clemente-Colón, P. Comparison of SAR-derived wind speed with model predictions and ocean buoy measurements. *IEEE Trans. Geosci. Remote Sens.* **2001**, *39*, 2587-2600.

19. Monaldo, F.; Thompson, D.R.; Pichel, W.; Clemente-Colón, P. A systematic comparison of QuickSCAT and SAR ocean surface wind speeds. *IEEE Trans. Geosci. Remote Sens.* **2004**, *42*, 283-291.
20. Capps, S.B.; Zender, C.S. Estimated global ocean wind power potential from QuikSCAT observations, accounting for turbine characteristics and siting. *J. Geophys. Res.* **2010**, *115*, DO09101.
21. Gash, J.H.C. A note on estimating the effect of a limited fetch on micrometeorological evaporation measurements. *Bound.-Layer Meteorol.* **1986**, *35*, 409-413.
22. Hasager, C.B.; Dellwik, E.; Nielsen, M.; Furevik, B. Validation of ERS-2 SAR offshore wind-speed maps in the North Sea. *Int. J. Remote Sens.* **2004**, *25*, 3817-3841.
23. Nielsen, M.; Astrup, P.; Hasager, C.B.; Barthelmie, R.J.; Pryor, S.C. *Satellite Information for Wind Energy Applications*; Risø-R-1479(EN); Risø National Laboratory: Roskilde, Denmark, 2004.
24. Troen, I.; Petersen, E.L. *European Wind Atlas*; Risø National Laboratory: Roskilde, Denmark, 1989.
25. Pryor, S.C.; Nielsen, M.; Barthelmie, R.J.; Mann, J. Can satellite sampling of offshore wind speeds realistically represent wind speed distributions? Part II Quantifying uncertainties associated with sampling strategy and distribution fitting methods. *J. Appl. Meteorol.* **2004**, *43*, 739-750.
26. Garratt, J.R. Review of drag coefficients over oceans and continents. *Month. Weather Rev.* **1977**, *105*, 915-929.
27. Antoniou, I.; Jørgensen, H.E.; Mikkelsen, T.; Frandsen, S.; Barthelmie, R.; Perstrup, C.; Hurtig, M. Offshore wind profile measurements from remote sensing instruments. In *European Wind Energy Conference and Exhibition 2006*, Athens, Greece, February 27–March 2, 2006; European Wind Energy Association: Brussels, Belgium, 2007; pp. 1-10.
28. Lange, B.; LARSEN, S.E.; Højstrup, J.; Barthelmie, R. Importance of thermal effects and sea surface roughness for offshore wind resource assessment. *J. Wind Eng. Ind. Aerodyn.* **2004**, *92*, 959-988.
29. Smedman, A.; Högström, U.; Bergstrom, H. The turbulence regime of a very stable marine airflow with quasi-frictional decoupling. *J. Geophys. Res.* **1997**, *102*, 21049-21059.
30. Mortensen, N.; Heathfield, D.N.; Landberg, L.; Rathmann, O.; TROEN, I.; Petersen, E.L. *Wind Atlas Analysis and Wind Atlas Analysis and Application Program: WAsP 7.0 Help Facility*; Risø National Laboratory: Roskilde, Denmark, 2000.
31. Koch, W. Directional analysis of SAR images aiming at wind direction. *IEEE Trans. Geosci. Remote Sens.* **2004**, *42*, 702-710.
32. Stoffelen, A.; Anderson, D.L.T. Scatterometer data interpretation: Estimation and validation of the transfer fuction CMOD4. *J. Geophys. Res.* **1997**, *102*, 5767-5780.
33. Barthelmie, R.; Badger, J.; Pryor, S.; Hasager, C.B.; Christiansen, M.B.; Jørgensen, B.H. Offshore coastal wind speed gradients: Issues for the design and development of large offshore windfarms. *Wind Eng.* **2007**, *31*, 369-382.
34. Barthelmie, R.; Pryor, S. Challenges in predicting power output from offshore wind. *J. Energy Eng.* **2006**, *132*, 91-103.

35. Barthelmie, R.; Courtney, M.; Nielsen, M. *The Wind Resource at Middelgrunden*; Risø National Laboratoy: Roskilde, Denmark, 1998.
36. Pryor, S.; Barthelmie, R. Statistical analysis of flow characteristics in the coastal zone. *J. Wind Eng. Ind. Aerodyn.* **2002**, *90*, 201-221.
37. Christiansen, M.B.; Hasager, C.B. Using airborne and satellite SAR for wake mapping offshore. *Wind Energy* **2006**, *9*, 437-455.
38. Sathe, A.; Gryning, S.-E.; Peña, A. Comparison of the Atmospheric Stability and Wind Profile Climatology at two Wind Farm Sites over a long marine fetch in the North Sea. *Wind Energy* **2010**, (in review).
39. Peña, A.; Hasager, C.B.; Gryning, S.E.; Courtney, M.; Antoniou, I.; Mikkelsen, T. Offshore wind profiling using light detection and ranging measurements. *Wind Energy* **2009**, *12*, 105-124.
40. Peña, A.; Gryning, S.E. Charnock's roughness length model and non-dimensional wind profiles over the sea. *Bound.-Layer Meteorol.* **2008**, *128*, 191-203.
41. Peña, A.; Gryning, S. E.; Hasager, C. B. Measurements and modelling of the wind speed profile in the marine atmospheric boundary layer. *Bound.-Layer Meteorol.* **2008**, *129*, 479-495.

Appendix 1

Table A. Offshore wind farms in operation, under construction and in planning: Number of turbines (T), wind farm capacity (Cap. in MW), geographical position (latitude and longitude), distance (D in km) from nearest coastline (from http://www.4coffshore.com/windfarms) and calculated wind statistics from satellite Envisat ASAR mean wind speed (U in m s^{-1}), Weibull A (m s^{-1}) and k (−), wind power density (E in W m^{-2})) and the number (N) of wind samples. Tables are given for Denmark (DK), Sweden (SE), Germany (DE) and Poland (PL).

DK	Wind farm	Year	T	Cap.	Lat. Long.	D	U	A	k	E	N
1	Vindeby	1991	11	4.9	54.97N 11.13E	1.8	6.79	7.60	1.66	461	469
2	Tunø Knob	1995	10	5	55.97N 10.36E	5.5	6.46	7.30	2.08	309	497
3	Middelgr.	2000	20	40	55.69N 12.68E	4.7	7.36	8.24	1.68	575	422
4	Rødsand I	2003	72	166	54.55N 11.71E	10.9	7.80	8.81	2.21	514	438
5	Samsø	2003	10	23	55.72N 10.58E	4.0	7.23	8.16	2.13	423	483
6	Fr.havn I	2003	3	7.6	57.43N 10.59E	2.2	6.84	7.65	1.67	468	520
7	Sprogø	2009	7	21	55.34N 10.96E	9.3	6.52	7.35	2.02	326	510
8	Avedøre	2010	3	11	55.60N 12.46E	0.4	6.46	7.26	1.79	360	484
9	Rødsand II	2010	90	207	54.56N 11.55E	8.6	7.22	8.15	2.05	437	442
10	Fr.havn. II	2012	6	36	57.46N 10.64E	7.9	7.01	7.86	1.71	489	527
11	Anholt P	2012		200	56.50N 11.28E	20.9	7.80	8.80	2.02	559	546
12	Anholt O	2012		200	56.62N 11.18E	18.2	7.86	8.87	1.92	604	549
13	GrenåHavn		3	18	56.42N 10.97E	2.6	6.99	7.89	2.04	400	509
14	KriegersFlakR			200	55.10N 12.81E	20.7	7.89	8.88	1.84	639	417
15	KriegersFlakS			200	55.00N 13.07E	33.4	8.15	9.20	1.99	647	385
16	KriegersFlakT			200	55.04N 12.98E	28.5	7.93	8.94	1.93	617	426
17	KriegersFlakU			200	54.93N 12.98E	27.5	7.92	8.93	1.87	634	420
18	RønneBankeX			200	54.95N 14.42E	23.4	8.36	9.38	1.75	802	419

Table A. *Cont.*

19	RønneBankeV			200	54.89N 14.29E	34	8.37	9.39	1.75	809	420
20	Stora Midlgr.Q			200	56.50N 12.04E	44	8.00	9.02	1.95	624	524
SE	**Wind farm**	**Year**	**T**	**Cap.**	**Lat. Long.**	**D**	**U**	**A**	**k**	**E**	**N**
1	Bockstigen	1998	5	3	57.04N 18.15E	5.8	7.08	7.97	1.86	456	442
2	Utgrunden I	2000	7	10	56.34N 16.28E	7.3	6.52	7.35	1.89	349	485
3	Ytre Stengr.	2001	5	10	56.17N 16.02E	3.7	6.62	7.45	1.89	364	459
4	Lillgrund	2007	48	110	55.51N 12.78E	9.3	7.73	8.70	1.86	592	419
5	Taggen	2012	83	300	55.86N 14.57E	16.3	7.09	7.99	1.88	453	436
6	KriegersFlakII	2015	128	640	55.07N 13.10E	32.4	7.95	8.95	1.83	657	407
7	StoraMiddelgr.	2016	108	540	56.61N 12.11E	34.3	7.96	8.98	1.97	610	525
8	Kårehamn	2016		50	56.98N 17.02E	7.0	6.59	7.43	1.93	354	482
9	Utgrunden II	2016	24	90	56.38N 16.27E	8.0	6.34	7.14	1.84	331	482
10	Blekinge	2019	500	2500	55.93N 15.02E	19.5	7.49	8.45	2.02	494	444
11	Trollboda		30	150	56.30N 16.18E	7.7	6.24	7.03	1.91	303	481
12	Södra Midsjö.			900	55.67N 17.27E	78.9	8.33	9.40	1.96	702	461
13	Klasarden		16	48	57.06N 18.16E	1.6	6.93	7.81	1.88	422	442
DE											
1	Breitling	2008	1	2.5	54.16N 12.13E	0.3	7.33	8.24	1.81	523	161
2	EnBW Baltic1	2010	21	48	54.61N 12.65E	17.1	7.44	8.38	1.84	537	435
4	VentotecOst2	2014	80	400	54.83N 14.07E	40.0	8.30	9.34	1.86	733	406
5	ArkonaBeck Süd.		80	400	54.78N 14.12E	37.6	8.17	9.19	1.83	679	407
6	GEOFReE		5	25	54.25N 11.40E	18.6	6.91	7.80	1.97	714	419
7	Beta Baltic		50	115	54.28N 11.40E	15.8	6.99	7.89	2.02	585	418
8	ArkoniaSee Sud		80	80	54.78N 13.87E	26.4	8.19	9.24	1.93	403	385
9	ArkoniaSee West		80	80	54.80N 13.80E	25.8	8.17	9.21	1.88	679	387
10	ArcadisOstI		70	350	54.83N 13.60E	20.0	8.15	9.18	1.83	690	409
11	ArcadisOst2		25	75	54.82N 14.13E	40.9	8.16	9.18	1.84	707	398
12	Baltic Eagle		80	480	54.83N 13.87E	30.8	8.25	9.31	1.96	707	386
13	BalticPower West		80	400	54.93N 13.08E	31.8	8.09	9.13	1.98	682	386
14	Baltic Power East		80	400	54.97N 13.24E	33.4	8.23	9.27	1.87	637	411
15	AldergrundNord.		31	155	54.85N 14.06E	40.2	8.25	9.29	1.87	718	405
16	Aldergrund GAP		31	186	54.82N 14.13E	40.9	8.16	9.18	1.84	707	398
17	Aldergrund 500		20	72	54.82N 14.1E	39.0	8.26	9.29	1.84	729	408
18	Arkona SeeOst			150	54.86N 14.02E	39.8	8.25	9.28	1.84	726	405
19	Beltsee		25	125	54.44N 11.51E	13.2	7.14	8.06	2.03	427	434
PL											
1	Poland P1			225	55.07N 16.64E	54.1	7.84	8.78	1.70	689	417
2	Poland P2			225	55.08N 16.9E	46.7	8.15	9.18	1.89	683	451
3	Poland P3			225	54.96N 18.21E	14.6	7.79	8.74	1.72	668	411
4	Poland P4			225	54.94N 18.37E	11.8	7.84	8.78	1.70	689	417